Crystal to Crystal Guest Exchange in a Mixed Ligand Metal−Organic Framework

Andrew P. Nelson,*,† Damon A. Parrish,‡ Lee R. Cambrea,† Lawrence C. Baldwin,† Nirupam J. Trivedi,† Karen L. Mulfort,§,# Omar K. Farha,§ and Joseph T. Hupp§

†Naval Air Warfare Center, Weapons Division, China Lake, California 93555, ‡Naval Research Laboratory, 4555 Overlook Avenue, Washington, DC 20375, and §Department of Chemistry and International Institute for Nanotechnology, Northwestern University, 2145 Sheridan Road, Evanston, Illinois 60208. # Current address: Division of Chemical Synthesis and Engineering, Argonne National Laboratory, Argonne, Illinois 60439.

ABSTRACT: The occluded solvent in a mixed ligand metal−organic framework has been displaced by *n*-hexanol, chloroform, and nitrobenzene in a crystal to crystal guest exchange. The X-ray structures of the three new solvent adducts of $Zn_2NDC_2DPNI_2$ reveal the complete replacement of N',N-dimethylformamide with the new guest. Structural changes to the framework geometry in response to the size of the incoming guest are also exhibited. These new frameworks are characterized by powder X-ray diffraction, thermal gravimetric analysis coupled with infrared spectroscopy, and cross-polarization magic angle spinning NMR.

Introduction. Metal−organic frameworks (MOFs) are an emerging class of porous materials with extremely high surface area.[1] These highly designable organic−inorganic hybrids are capable of a variety of applications, such as chemical separations,[2] catalysis,[3] fuel storage,[4] and small molecule preconcentration.[5] In many cases, MOFs are prepared with multiple levels of network interpenetration as well as labile ligands which can lead to frameworks with dynamic structures.[6] In most cases, the dynamic nature of these coordination networks is exposed by removal of the occluded solvents, followed by resolution or by simple exchange of one small molecule guest for another. Recently, Hupp and others have reported the preparation and electronic manipulation of a series of mixed ligand MOFs whose structures exhibit multiple levels of interpenetration.[7] Here we report dynamic framework behavior observed during the single crystal to single crystal guest exchange of one of these mixed ligand frameworks, namely, $Zn_2NDC_2DPNI \cdot DMF$ (Figure 1), where NDC is the dianion of 1,6-napthalene dicarboxylic acid, DPNI is N',N-di-(4-pyridyl)1,4,5,8-napthalenetetracarboxydiimide, and DMF is N',N-dimethylformamide, which is employed as a reaction medium, and is occluded as a result of the framework synthesis. In this study, we report dynamic changes to the framework geometry and pore size in response to the size of the incoming guest.

Experimental Section. General Information. Commercial reagents were purchased from Sigma-Aldrich (ACS grade) and used as received. Powder X-ray diffraction patterns were recorded with a PANalytical X'Pert PRO, X-ray diffraction system utilizing a lightweight ceramic X-ray tube with a Copper Anode. Fourier transform infrared (FTIR) analysis was performed using a Nicolet Nexus 870 FTIR spectrometer with a TA Instruments 2050 TGA interfaced with a heated cell and transfer line. Single crystals were mounted on a Bruker three-circle platform diffractometer equipped with a SMART APEX II CCD detector. The crystals were irradiated using graphite monochromated Mo Kα radiation ($\lambda = 0.71073$). An MSC X-Stream low temperature device was used to keep the crystals at a constant 113(2) K during data collection. All solid-state ^{13}C CPMAS NMR experiments were obtained at room temperature and conducted on a Bruker Advance 200 MHz spectrometer at 50 MHz. Samples were spun at 7 kHz, using 4 mm ZrO_2 rotors

with Kel-F caps in a standard Bruker 4 mm CPMAS probe. The number of transients for the solid-state spectra ranged from 5 k to 10 k with a 5 s recycle delay between scans. Solution state ^{13}C NMR experiments were conducted on a Bruker Advance 300 MHz spectrometer at 75 MHz. Single crystal and bulk samples of $Zn_2NDC_2DPNI \cdot DMF$ (**1**) were prepared according to the published procedures.[7]

Solvent Exchange Reactions. All solvent exchanged reactions were performed on freshly prepared samples of **1**. For the single crystal to single crystal exchanges, and equal volume of the exchanging solvent was carefully layered on top of the single crystals of **1** still solvated by the preparative $DMF/Zn(NO_3)_2 \cdot 6H_2O/NDC/DPNI$ solution. The $DMF/Zn(NO_3)_2 \cdot 6H_2O/NDC/DPNI$ portion of the new solution was immediately removed and replaced by another portion of the exchanging solvent. This procedure was repeated three times during the initial exposure to the exchanging solvent. The procedure was repeated every 24 h for 2 weeks being careful to keep the MOF crystals fully solvated at all times. Bulk samples of **2**, **3**, and **4** were prepared from freshly prepared bulk samples of **1** that had previously been isolated by filtration, washed with DMF, and dried in the air for 30 min. These bulk samples of **1** were soaked in neat hexanol, chloroform, and nitrobenzene, respectively. For the bulk samples, the exchanging solvent was removed by pipet and replaced with fresh solvent every 24 h for 2 weeks.

Results and Discussion. The mixed ligand framework $Zn_2NDC_2DPNI_2 \cdot nDMF$ (**1**) was chosen for its ease of preparation, available pore size, and the large size of prepared crystals. The large yellow crystals are excellent candidates for single crystal X-ray analysis and continue to scatter X-rays well following guest exchange over the course of several weeks. In addition, a larger scale preparation of this material has recently been reported.[7b]

Crystal to crystal guest exchange was accomplished by layering an equal volume of the exchanging solvent on top of the single crystals of **1** still immersed in the reaction solvent (DMF). The reaction solvent was then removed from the reaction vessel, paying careful attention to keep the crystals solvated at all times, and replaced by another equal volume addition of the exchange solvent. This procedure was repeated three times during the initial introduction of the MOF to the incoming guest and then once every 24 h for 2 weeks. Crystals of **1** exposed to 1-hexanol, chloroform, and nitrobenzene show no visual changes to crystal size or morphology and only slight variation of their yellow color.

---

*Corresponding author. E-mail: andrew.p.nelson@navy.mil.

After exposure to the exchanging solvents the crystals were analyzed by single crystal X-ray diffraction to reveal three new
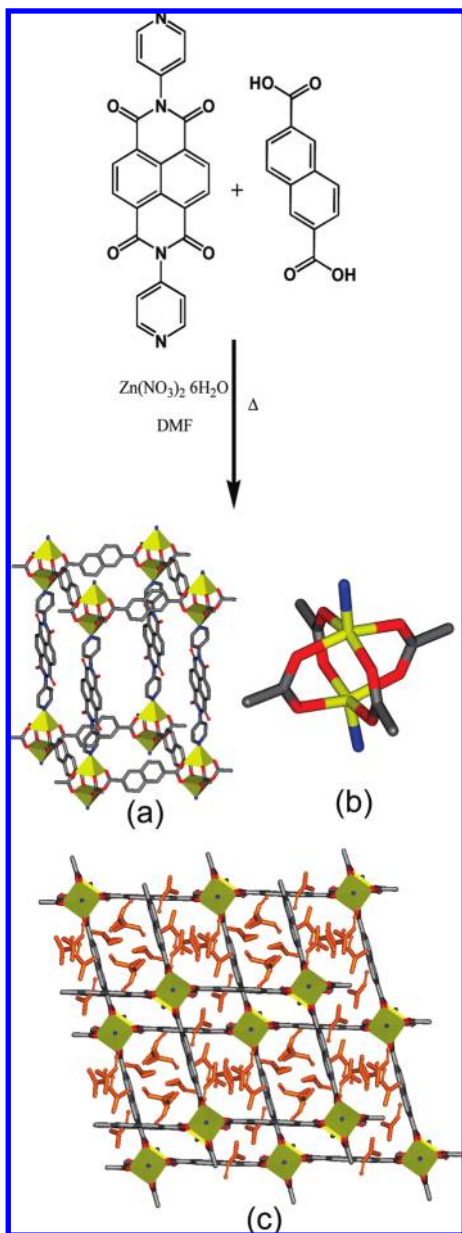

Figure 1. Preparation of and crystallographically derived: (a) structure of $Zn_2(NDC)_2DPNI \cdot nDMF$, **1**, in which the occluded DMF molecules and interpenetrated framework have been removed, (b) corner cluster showing coordination modes of **1**, (c) *ac* plane of **1**, looking down the *b*-channels in which the occluded DMF molecules have been rendered completely orange.

structures $Zn_2NDC_2DPNI_2 \cdot C_5H_{13}OH$ (**2**), $Zn_2NDC_2DPNI_2 \cdot CHCl_3$ (**3**), and $Zn_2NDC_2DPNI_2 \cdot C_6H_5NO_2$ (**4**). Crystal data for the new structures is listed in Table 1. In each case, the new structures reveal the complete exchange of the DMF for the new guest, as well as significant changes to framework geometry. The most notable change as the frameworks shift to accommodate guest molecules of different sizes is a lateral movement of atoms along the framework axes defined by the NDC ligands. The structural variation of the framework upon guest exchange is comparatively illustrated in Figure 2. Shown here, looking down the axis defined by the DPNI ligands at an isolated framework unit of each of the three new MOFs as well as **1**, we can see that the framework adopts a rhombohedral shape when solvated by the smaller hexanol and chloroform molecules and a more cubic geometry when accommodating the larger nitrobenzene guests.

It has been postulated that in these types of interpenetrating networks, structural rearrangements arise from the movement of the entangled cages with respect to one another.[8] In this system, however, the distance between the entangled frameworks at their closet point remains roughly 3.5 Å, varying by less than one tenth of an angstrom from one structure to the next. This relatively
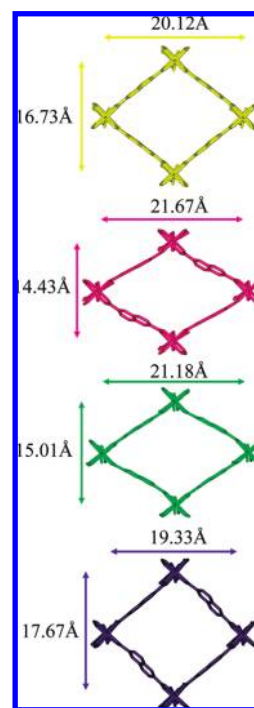

Figure 2. View of the pore systems of individual frameworks of $Zn_2(NDC)_2DPNI \cdot DMF$, **1** (yellow), $Zn_2(NDC)_2DPNI \cdot C_6H_{13}OH$, **2** (pink), $Zn_2(NDC)_2DPNI \cdot CHCl_3$, **3** (green), and $Zn_2(NDC)_2DPNI \cdot C_6H_5NO_2$, **4** (purple). Guest solvent molecules and interpenetrated framework units have been removed for clarity.

Table 1. Crystal Data for Guests Exchanged Frameworks

designation	$Zn_2(NDC)_2DPNI \cdot DMF$ (**1**)[a]	$Zn_2(NDC)_2DPNI \cdot C_6H_{13}OH$ (**2**)	$Zn_2(NDC)_2DPNI \cdot CHCl_3$ (**3**)	$Zn_2(NDC)_2DPNI \cdot C_6H_5NO_2$ (**4**)
formula	$C_{67.50}H_{69.50}N_{10.50}O_{18.50}Zn_2$	$C_{64.50}H_{61.95}N_4O_{14.75}Zn_2$	$C_{49.25}H_{25.25}Cl_{3.75}N_4O_{12}Zn_2$	$C_{74.78}H_{46.32}N_{8.46}O_{20.92}Zn_2$
crystal system	monoclinic	triclinic	monoclinic	monoclinic
space group	$P2_1$	$P\bar{1}$	$P2_1$	$P2_1$
a (Å)	12.993(13)	12.975(2)	12.972(4)	13.063(2)
b (Å)	22.318(2)	13.060(2)	22.296(7)	22.324(4)
c (Å)	13.090(13)	22.382(4)	12.988(4)	13.129(2)
α (°)	90	95.776(2)	90	90
β (°)	102.582(2)	92.004(3)	109.376	95.149(3)
γ (°)	90	112.678(2)	90	90
cell volume (Å)	3705.1(6)	3470.5(9)	3543.6(19)	3813.2(11)

[a] Data taken from ref 7a.

small variation is in contrast to the greater than 3 Å difference for the closest diagonal Zn−Zn through space distance in changing from the largest guest, nitrobenzene to the smallest, *n*-hexanol. The lateral shift in the frameworks' *xy* plane is reminiscent of the breathing effects shown by Ferey in their MIL-53 frameworks[6a] as well as the dynamic behavior reported by Kaskel.[6k]

The guest exchanged complexes were characterized by powder X-ray diffraction (PXRD), thermal gravimetric analysis coupled with infrared spectroscopy (TGA-IR), and solid-state ^{13}C cross-polarization magic angle spinning (CPMAS) NMR. In each case, the PXRD traces for bulk samples of guest exchanged MOFs match the simulated traces generated from the single crystal X-ray structure (see Supporting Information). The TGA data of **2**, **3**, and **4** indicate calculated mass decreases 33%, 8%, and 38% respectively, results that are consistent with the X-ray structures. Figure 3 shows the time-resolved FTIR spectra taken while heating **2** at a rate of 10 deg/min. Spectra were not corrected for water and carbon dioxide, so these bands are observed throughout the heating cycle. For each sample, the first product observed corresponds to the exchanged guest. The identity of the liberated products, *n*-hexanol, chloroform, and nitrobenzene, was confirmed by comparison to the IR trace of the pure material (see Supporting Information). Following the liberation of the adsorbed guest, the next peaks in the IR traces are identical and appear around the 40-min mark or approximately 400 °C. These peaks most closely resemble the IR spectra of naphthalene accompanied by the large increase in CO_2 released, both indicative of framework decomposition.

An example of guest inclusion characterized by CPMAS NMR is illustrated by the spectra shown in Figure 4. The presence of the hexanol peak resonances from the CPMAS experiment of the impregnated sample clearly indicates adsorption to the MOF.
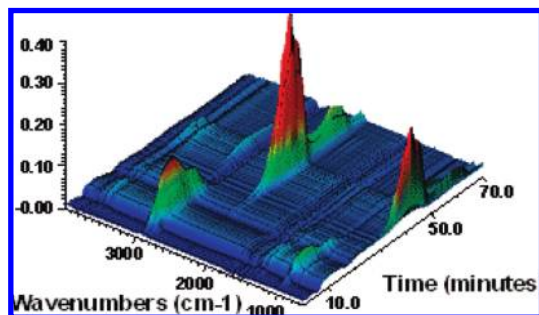
Figure 3. Time resolved TGA-IR of **2** showing the loss of occluded *n*-hexanol ∼ 1−30 min followed by CO_2 and naphthalene ∼ 40 min.
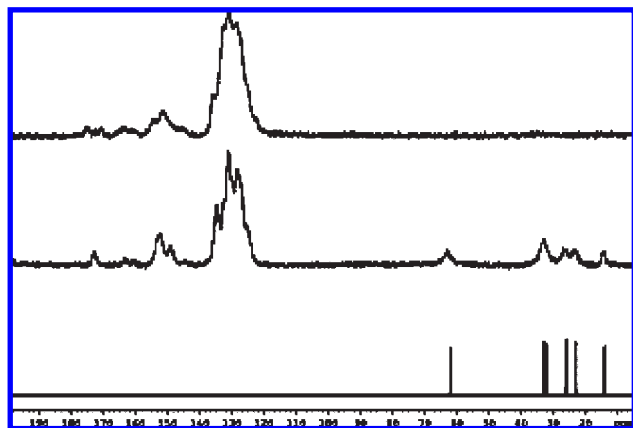
Figure 4. CPMAS NMR of **1** following removal of the DMF by vacuum extraction (top). CPMAS NMR of **2** following hexanol exchange of **1** (middle). Solution ^{13}C NMR spectra of hexanol (bottom).

Furthermore, because CPMAS will only show resonances that are from solids or from molecules that have very low mobility, we see that exposing hexanol as well as other guests to the caged MOF structure significantly restricts the guests' mobility, indicative of guest occlusion within the porous framework. The top spectrum shows the ^{13}C CPMAS of **1** in which the preparative DMF has been evacuated. The aromatic ringed carbons primarily are located in the broad pattern from 120 to 140 ppm. The pyridine ring carbons are near 150 ppm, and the carbonyl carbons are from roughly 155 and above. When hexanol is introduced, peaks at 14, 22.9, 25.9, 32.1, 32.8, and 62 ppm appear, corresponding to the adsorbed hexanol carbon resonances. A solution-state spectrum of hexanol is shown for comparison. Changes to the peak pattern from 120 to 140 ppm indicate a change in the environment of the MOF, likely caused by the exchange of DMF in favor of hexanol. The CPMAS NMR analysis of **3** and **4** also indicates complete exchange of DMF for nitrobenzene and chloroform, respectively (see Supporting Information).

To test the reversibility of the solvent exchange process, single crystals of **2**, **3**, and **4** were soaked in DMF for a period of 4 weeks. The PXRD spectra taken after the resolution in DMF are indistinguishable from the spectra of newly prepared **1**. Single crystals of **3** were analyzed by single crystal X-ray diffraction. The unit cell for the exchanged and resolvated crystals matched the dimensions of the previously published DMF solvated structure. Therefore, it appears that the structural rearrangement due to guest exchange is reversible.

Conclusions. To summarize, we have shown the single crystal to single crystal exchange of three separate occluded guests in a mixed ligand MOF. The complete exchange of the reagent solvent for the new guests has been verified by TGA-IR. During the guest exchange, the framework geometry is dynamic and reversible, changing in response to the size of the incoming guest.

Supporting Information Available: X-ray crystallographic files for **2**, **3**, and **4** in CIF format, additional PXRD, TGA, TGA-IR, and CMAS NMR data. This material is available free of charge via the Internet at http://pubs.acs.org.

References

(1) Recent reviews: (a) Collins, D. J.; Zhou, H.-C. *J. Mater. Chem.* **2007**, *17*, 3154–3160. (b) Fe'rey, G. *Chem. Soc. Rev.* **2008**, *37*, 191–214.

(2) For example, see: (a) Bastin, L.; Barcia, P. S.; Hurtado, E. J.; Silva, J. A. C.; Rodrigues, A. E.; Chen, B. *J. Phys. Chem. C* **2008**, *112*, 1575–1581. (b) Lee, E. Y.; Jang, S. Y.; Suh, M. P. *J. Am. Chem. Soc.* **2005**, *127*, 6374–6381. (c) Dinca, M.; Long, J. R. *J. Am. Chem. Soc.* **2005**, *127*, 9376–9377. (d) Snurr, R. Q.; Hupp, J. T.; Nguyen, S. T. *AIChE* **2004**, *50*, 1090–1095. (e) Bae, Y. S.; Mulfort, K. L.; Frost, H.; Ryan, P.; Punnathanam, S.; Broadbelt, L. J.; Hupp, J. T.; Snurr, R. Q. *Langmuir* **2008**, *24*, 8592–8598. (f) Bae, Y. S.; Farha, O. K.; Spokoyny, A. M.; Mirkin, C. A.; Hupp, J. T.; Snurr, R. Q. *Chem. Commun.* **2008**, 4135–4137. (g) Li, J.-R.; Kuppler, R. J.; Zhou, H.-C. *Chem. Soc. Rev.* **2009**, *38*, 1477–1504. (h) Bae, Y.-S.; Farha, O. K.; Hupp, J. T.; Snurr, R. Q. *J. Mater. Chem* **2009**, *19*, 2131–2134.

(3) Wu, C.-D.; Hu, A.; Zhang, L.; Lin, W. *J. Am. Chem. Soc.* **2005**, *127*, 8940–8941. Horike, S.; Dinca, M.; Tamaki, K.; Long, J. R. *J. Am. Chem. Soc.* **2008**, *130*, 5854–5855. Cho, S.-H.; Ma, B.; Nguyen, S. T.; Hupp, J. T.; Albrecht-Schmitt, T. E. *Chem. Commun.* **2006**, *256*, 3–2565. Lee, J.-Y.; Farha, O. K.; Roberts, J.; Scheidt, K. A.; Nguyen, S. T.; Hupp, J. T. *Chem. Soc. Rev.* **2009**, *38*, 1450–1459.

(4) For example, see: (a) Collins, D. J.; Zhou, H.-C. *J. Mater. Chem.* **2007**, *17*, 3154–3160. (b) Fe'rey, G. *Chem. Soc. Rev.* **2008**, *37*, 191–214. (c) Nouar, F.; Eubank, J. F.; Bousquet, T.; Wojtas, L.; Zaworotko,

M. J.; Eddaoudi, M. *J. Am. Chem. Soc.* **2008**, *130*, 1833–1835. (d) Chen, B.; Ockwig, N. W.; Millard, A. R.; Contreras, D. S.; Yaghi, O. M. *Angew. Chem., Int. Ed.* **2005**, *44*, 4745–4749. (e) Dinca, M.; Dailly, A.; Liu, Y.; Brown, C. M.; Neumann, D. A.; Long, J. R. *J. Am. Chem. Soc.* **2006**, *128*, 16876–16883. (f) Latroche, M.; Surble′, S.; Serre, C.; Mellot-Draznieks, C.; Llewellyn, P. L.; Lee, H.; Chang, J.; Jhung, S. H.; Fe′rey, G. *Angew. Chem., Int. Ed.* **2006**, *45*, 8227–8231. (g) Mulfort, K. L.; Hupp, J. T. *J. Am. Chem. Soc.* **2007**, *129*, 9604–9605. (h) Farha, O. K.; Spokoyny, A. M.; Mulfort, K. L.; Hawthorne, M. F.; Mirkin, C. A.; Hupp, J. T. *J. Am. Chem. Soc.* **2007**, *129*, 12680–12680. (i) Farha, O. K.; Mulfort, K. L.; Hupp, J. T. *Inorg. Chem.* **2008**, *47*, 10223–10225.

(5) Ni, Z.; Jerrell, J. P.; Cadwallader, K. R.; Masel, R. I. *Anal. Chem.* **2007**, *79*, 1290–1293.

(6) For example see: (a) Serre, C.; Millange, F.; Thouvenot, C.; Nogues, M.; Marsolier, G.; Louer, D.; Ferey, G. *J. Am. Chem. Soc.* **2002**, *124*, 13519–13526. (b) Barthelet, K.; Marrot, J.; Riou, D.; Ferey, G. *Angew. Chem., Int. Ed.* **2002**, *41*, 281. (c) Loiseau, T.; Serre, C.; Huguenard, C.; Fink, G.; Taulelle, F.; Henry, M.; Bataille, T.; Ferey, G. *Chem.—Eur. J.* **2004**, *10*, 1373–1382. (d) Mellot-Draznieks, C.; Serre, C.; Surble, S.; Audebrand, N.; Ferey, G. *J. Am. Chem. Soc.* **2005**, *46*, 16273–16278. (e) Dybtsev, D. N.; Chun, H.; Kim, K. *Angew. Chem., Int. Ed* **2004**, *43*, 5033–5036. (f) Kitagawa, S.; Uemura, K. *Chem. Soc. Rev.* **2005**, *34*, 109–119. (g) Fletcher, A. J.; Thomas, K. M.; Rosseinsky, M. J. *J. Solid State Chem.* **2005**, *178*, 2491–2510. (h) Uemura, K.; Matsuda, R.; Kitigawa, S. *J. Solid State Chem.* **2005**, *178*, 2420–2429. (i) Kasai, K.; Fujita, M. *Chem.—Eur. J.* **2007**, *13*, 3089–3105. (j) Zhao, J.; Long, L. S.; Huang, R. B.; Zheng, L. S. *Dalton Trans.* **2008**, *35*, 4714–4716. (k) Senkovska, I.; Kaskel, S. *Eur. J. Inorg. Chem.* **2006**, 4564–4569.

(7) (a) Ma, B. Q.; Mulfort, K. L.; Hupp, J. T. *Inorg. Chem.* **2005**, *44* (14), 4912–4914. (b) Mulfort, K. L.; Hupp, J. T. *J. Am. Chem. Soc.* **2007**, *129* (31), 9604–9605. (c) Mulfort, K. L.; Hupp, J. T. *Inorg. Chem.* **2008**, *47*, 7936–7938.

(8) Chen, B.; Ma, S.; Zapata, F.; Lobkovsky, E. B.; Yang, J. *Inorg. Chem.* **2006**, *45*, 5718–5720.